THE JOURNAL OF BIOLOGICAL CHEMISTRY
Vol. 280, No. 19, Issue of May 13, pp. 19250–19258, 2005
Printed in U.S.A.

Structural Basis for the Cell-specific Activities of the NGFI-B and the Nurr1 Ligand-binding Domain*

Received for publication, November 22, 2004, and in revised form, February 3, 2005
Published, JBC Papers in Press, February 16, 2005, DOI 10.1074/jbc.M413175200

Ralf Flaig‡§, Holger Greschik‡, Carole Peluso-Iltis, and Dino Moras¶

From the Département de Biologie et Génomique Structurales, IGBMC, CNRS/INSERM/ULP, 1 Rue Laurent Fries, B.P. 10142, Illkirch 67404, France

NGFI-B is a ligand-independent orphan nuclear receptor of the NR4A subfamily that displays important functional differences with its homolog Nurr1. In particular, the NGFI-B ligand-binding domain (LBD) exhibits only modest activity in cell lines in which the Nurr1 LBD strongly activates transcription. To gain insight into the structural basis for the distinct activation potentials, we determined the crystal structure of the NGFI-B LBD at 2.4-Å resolution. Superimposition with the Nurr1 LBD revealed a significant shift of the position of helix 12, potentially caused by conservative amino acids exchanges in helix 3 or helix 12. Replacement of the helix 11–12 region of Nurr1 with that of NGFI-B dramatically reduces the transcriptional activity of the Nurr1 LBD. Similarly, mutation of Met^{414} in helix 3 to leucine or of Leu^{591} in helix 12 to isoleucine (the corresponding residues found in NGFI-B) significantly affects Nurr1 transactivation. In comparison, swapping the helix 11–12 region of Nurr1 into NGFI-B results in a modest increase of activity. These observations reveal a high sensitivity of LBD activity to changes that influence helix 12 positioning. Furthermore, mutation of hydrophobic surface residues in the helix 11–12 region (outside the canonical co-activator surface constituted by helices 3, 4, and 12) severely affects Nurr1 transactivation. Together, our data suggest that a novel co-regulator surface that includes helix 11 and a specifically positioned helix 12 determine the cell type-dependent activities of the NGFI-B and the Nurr1 LBD.

In humans, the NR4A subfamily of nuclear receptors (NRs)[1] comprises three members: NGFI-B (NR4A1), Nurr1 (NR4A2), and NOR1 (NR4A3) (1–3). The *Drosophila* ortholog of NGFI-B is DHR38 (4). Monomeric, homodimeric, or heterodimeric NGFI-B, Nurr1, and NOR-1 regulate target gene transcription from target sequences such as AAAGGTCA, termed NGFI-B response elements (5, 6). In addition, NGFI-B and Nurr1 act on DR5 elements (AGGTCA NNNAA AGGTCA) as heterodimers with RXR (7, 8), a common dimerization partner of NRs, whereas NOR-1 fails to form stable RXR heterodimers (9). NGFI-B, Nurr1, and NOR-1 activate transcription in a cell type- and promoter-dependent manner (2, 3, 10–12). In heterodimers, agonist-bound RXR contributes to transcriptional activation (7, 8).

NGFI-B is expressed in various tissues, notably the brain, and plays a role in multiple cellular events such as cell proliferation, differentiation, and apoptosis (13–15). The receptor has been implicated in neurodegenerative pathologies, such as Parkinson disease, manic depression, and schizophrenia (16). Nurr1 is almost exclusively expressed in brain, is essential for the development of midbrain dopaminergic neurons, and accordingly is also linked to Parkinson disease (17–19). NOR-1 has been isolated from cultured forebrain neurons undergoing apoptosis (20) and plays a role in brain development but also acts in other tissues outside the central nervous system (14, 15).

NRs typically contain two activation functions, one located in the N-terminal domain, termed AF1, and the other found in the ligand-binding domain (LBD), termed AF2. For the NR4A subfamily, the AF1 appears to play the predominant role in transcriptional activation and co-factor recruitment, and its activity can be regulated by phosphorylation (21–26). Recent results show that the AF1 directly recruits co-activators such as members of the SRC family, p300, pCAF, and DRIP205 (25, 26). In comparison, the AF2 of NR4A receptors appears to be cell type-dependent, and significant differences have been observed for the transactivation efficiencies of Nurr1, NGFI-B, and NOR-1 (12). Importantly, the AF2 does not directly interact with SRCs, p300, pCAF, or DRIP205, and little is known about the regulation of its activity (12, 25, 27, 28). However, the co-repressor SMRT, the atypical orphan receptor DAX-1, and the SUMO ubiquitin ligase PIASγ have been reported to interact with the LBD of either NGFI-B or Nurr1, and play a role in AF2 regulation (22, 29, 30).

Structural studies have shown that the LBD of NRs adopts a canonical fold mainly composed of 12 α-helices (H1–H12) (31). In the case of the classical NRs, the LBD undergoes significant conformational changes upon the binding of an agonist ligand, which leads to a repositioning of the "activation helix" (H12). These changes generate a hydrophobic co-activator binding cleft constituted by H3, H4, and H12, to which L*XX*LL-containing co-activators, such as SRCs, p300, or DRIP205, bind. The L*XX*LL region adopts an α-helical conformation with the leucine residues forming critical contacts with the hydrophobic

* This work was supported by Université Louis Pasteur de Strasbourg, le Centre National de la Recherche Scientifique, l'Institut National de la Santé et da la Recherche Médicale, and in part by a Marie-Curie individual fellowship (to H. G.). The work described here was funded by the European Commission as SPINE, contract number QLG2-CT-2002–00988, under the RTD program "Quality of Life and Management of Living Resources." The costs of publication of this article were defrayed in part by the payment of page charges. This article must therefore be hereby marked "*advertisement*" in accordance with 18 U.S.C. Section 1734 solely to indicate this fact.

The atomic coordinates and structure factors (code 1YJE) have been deposited in the Protein Data Bank, Research Collaboratory for Structural Bioinformatics, Rutgers University, New Brunswick, NJ (http://www.rcsb.org/).

‡ These two authors contributed equally to this work.

§ Present address: Diamond Light Source Ltd., Rutherford Appleton Laboratory, Chilton, Didcot, Oxon OX11 0QX, United Kingdom.

¶ To whom correspondence should be addressed. Tel.: 33-3-88-65-32-20; Fax: 33-3-88-65-32-76; E-mail: moras@igbmc.u-strasbg.fr.

[1] The abbreviations used are: NR, nuclear receptor; LBD, ligand-binding domain; AF, activation function; AU, asymmetric unit; H, α-helix; BisTris, 2-[bis(2-hydroxyethyl)amino]-2-(hydroxymethyl)propane-1,3-diol; RXR, retinoid X receptor; RAR, retinoic acid receptor.

LBD surface. The co-activator helix is further positioned by a "charge clamp" interaction with a lysine in H3 and a glutamic acid in H12, conserved in most NR LBDs (32, 33).

The NR4A subfamily is significantly different to the classical NRs described above. First, structure determination of the LBDs of Nurr1 and DHR38 revealed a class of ligand-independent NRs, whose putative ligand-binding pocket is filled with bulky aromatic and hydrophobic residues (27, 28). Next, in members of the NR4A subfamily, the conserved lysine in H3 is replaced by a glutamic acid, whereas the glutamic acid in H12 is replaced by a lysine residue (with the exception of an asparagine in H12 of DHR38) (12). Finally, in addition to this "inversed" charge clamp, the canonical co-activator cleft constituted by H3, H4, and H12 has a hydrophilic rather than hydrophobic topology, explaining the lack of binding of known L*XX*LL-containing co-activators (25, 27).

Nevertheless, mutagenesis studies provided evidence that H12 is essential for the cell type-dependent AF2 activity of NR4A receptors (11, 12, 34). Further studies also showed that the putative co-activator cleft constituted by H3, H4, and H12 does not play a role in co-activator recruitment and suggested that Nurr1 activity is correlated with regulated, ligand-independent stabilization of the Nurr1 LBD (27). However, from these results, the question about a direct involvement of H12 in transactivation and the location of the co-regulator surface remained elusive.

Here we report the crystal structure of the rat NGFI-B LBD at 2.4-Å resolution. The NGFI-B LBD adopts an active conformation, and the putative ligand-binding pocket is filled with bulky aromatic and hydrophobic side chains as observed for the LBD crystal structures of Nurr1 and DHR38 (27, 28). Overall, the LBDs of NGFI-B and Nurr1 superimpose well with the exception of a significantly shifted H12 (about 2.8 Å). Structure comparison suggests that conserved amino acid exchanges in H3 or H12 partly account for the distinct H12 positions. Swapping the entire H11-H12 region of NGFI-B into Nurr1 reduces the AF2 activity of Nurr1 to NGFI-B levels, whereas the reverse swap results in a modest increase in activity of the NGFI-B LBD. Mutation of individual residues in H3 or H12 of Nurr1 to the corresponding residues of NGFI-B (mutant M414L or L591I, respectively) significantly reduces the cell type-dependent activity of the Nurr1 LBD. Finally, mutation of hydrophobic surface residues in the H11-H12 region severely affects Nurr1 transactivation. Together, these data provide evidence that a specific H12 position and a novel co-regulator surface determine the cell type-dependent AF2 activities of NGFI-B and Nurr1.

EXPERIMENTAL PROCEDURES

Recombinant Plasmids—The cDNAs encoding the LBDs of human Nurr1 (Swiss-Prot accession number P43354) and rat NGFI-B (Swiss-Prot accession number P22829) cloned in pET-15b (Novagen) are gifts from Hiroshi Ichinose. Wild-type or mutant cDNA fragments encoding the Nurr1 LBD (residues 362–598) or NGFI-B LBD (residues 354–597) were generated by PCR and cloned into the eukaryotic expression plasmid pCMX-Gal4. From pCMX-Gal4, the respective cDNA is expressed in fusion with the Gal4 DNA-binding domain (residues 1–147). Details of the cloning of these plasmids are available upon request. The plasmids pCMX-RXRα and pCMX-VP16-RXRα (resulting in expression of full-length human RXRα in fusion with the VP16 activation domain) were gifts from Roland Schüle.

Cell Culture and Transient Transfection—COS-1 cells were cultured in Dulbecco's modified Eagle's medium supplemented with 5% fetal calf serum and gentamycin. Transient transfection assays were carried out using the standard calcium phosphate co-precipitation technique in 24-well plates (Greiner) with 0.5×10^5 cells/well. Cells were transfected with 250 ng of $Gal4_{(3\times)}$-TK-LUC reporter plasmid (containing three Gal4 binding sites in front of the thymidine kinase promoter and the firefly luciferase reporter), 100 ng of pCH110 encoding β-galactosidase (Amersham Biosciences), and 25 ng or 100 ng of wild-type or mutant pCMX-Gal4-NGFI-B or pCMX-Gal4-Nurr1 expression plasmid per well. The empty plasmid pCMX-Gal4 served as control. Co-transfection experiments involving RXRα expression plasmids were carried out with 25 ng of wild-type or mutant pCMX-Gal4-Nurr1 and 75 or 150 ng of pCMX-RXRα (in the absence or presence of 10^{-8} M RXR agonist BMS649) or pCMX-VP16-RXRα per well. Cells were lysed with passive lysis buffer (Promega). Luciferase activity was measured in a Luminometer MicroLumat LB96P (EG&G Berthold) according to the manufacturer's instructions and normalized to β-galactosidase activity according to a standard protocol. All experiments were repeated at least three times.

Protein Production and Purification—The hexahistidine-tagged rat NGFI-B LBD (residues 354–597; 29,227 Da including tag) was produced from pET-15b (Novagen) in *Escherichia coli* BL21(DE3) at 37 °C in LB medium supplemented with 100 μg/ml ampicillin. After sonication of the bacterial pellet and ultracentrifugation, the recombinant protein was first purified by nickel affinity chromatography using a HiTrap chelating column (Amersham Biosciences) equilibrated with buffer A (20 mM Tris-HCl (pH 8.0), 200 mM NaCl, 5 mM imidazole) on a BioLogic work station (Bio-Rad) at 4 °C. After three wash steps of the resin with buffer A, the protein was eluted by increasing the imidazole concentration to 200 mM and then further purified by gel filtration using a HiLoad 16/60 Superdex 200 column (Amersham Biosciences). The NGFI-B LBD monomer eluted in buffer B (20 mM Tris-HCl (pH 8.0), 100 mM NaCl, 5 mM dithiothreitol) from the gel filtration column at the expected position as a single peak. The fractions containing purified protein (estimated purity from silver-stained SDS gels >95%) were pooled and concentrated to about 6 mg/ml. The correct mass was confirmed by electrospray ionization mass spectrometry under denaturing conditions.

Protein Crystallization, Data Collection, and Processing—Crystallization of the NGFI-B LBD (concentrated to about 6 mg/ml in buffer B) was carried out with the sitting drop vapor diffusion method in 96-well CrystalQuick™ plates (Greiner) (1.5 μl of protein solution plus 1.5 μl of reservoir against 150 μl of reservoir) using a Tecan Work station 150. Diffraction quality crystals were found using the Index™ screen (Hampton Research). Refinement of crystallization conditions was attempted but did not yield better quality crystals with respect to the initial condition. Crystals grew within a few days in sitting drops at 17 °C with a reservoir containing 3.0 M NaCl and 0.1 M BisTris (pH 5.5) and were cryoprotected in dried paraffin oil. X-ray diffraction data were collected at the Swiss Light Source (Villigen, Switzerland). The data were integrated and scaled using the XDS program package (35).

Structure Determination, Refinement, and Comparison—The crystal structure of the NGFI-B LBD was solved by molecular replacement with AMoRe (36) using a monomeric subunit of DHR38 (Protein Data Bank code 1PDU) as a search model and refined to 2.4-Å resolution using the CNS (37) and CCP4 program packages (38–41). Manual adjustment and rebuilding of residues was done with the program O (42). The final model was validated with PROCHECK (43) and comprises residues 362–541 and 549–594. Data collection and structure refinement statistics are summarized in Table I. For structure comparison the Cα traces of the NGFI-B, Nurr1 (Protein Data Bank code 1OVL), and DHR38 models were superimposed either completely or partially from the beginning of H1 to the end of H11 (residues 362–578 in NGFI-B, 363–579 in Nurr1, and 321–532 in DHR38) using the lsq commands of O and default parameters. Partial superimpositions were chosen to exclude the significantly shifted H12 from the calculation of the root mean square deviation. The figures were generated with Pymol (44) (available on the World Wide Web at www.pymol.org) and TeXshade (45).

RESULTS

Overall Structure of the NGFI-B LBD—The NGFI-B LBD adopts the canonical three-layered α-helical sandwich fold with H12 in an active position (Fig. 1*A*). As expected from sequence homology with Nurr1 and DHR38 (27, 28), no ligand-binding pocket is present. Instead, the space is filled with bulky aromatic or hydrophobic residues (Phe^{405} (H3), Leu^{409} (H3), Leu^{443} (H5), Phe^{446} (H5), Phe^{478} (loop H6-H7), and Trp^{481} (H7)) conserved within the NR4A subfamily (Fig. 1*B*).

The LBDs of NGFI-B and its *Drosophila* ortholog DHR38 superimpose well in most parts with a root mean square deviation of 1.16 Å over 215 atoms (1.14 Å over 199 atoms for superimposition from H1 to H11). We note a certain degree of

TABLE I
Data collection and refinement statistics

Parameters	Values
Space group	$I4_122$
Molecules/AU	1
Unit cell (Å)	$a = 90.422$; $b = 90.422$; $c = 140.637$ $\alpha = \beta = \gamma = 90°$
Data collection	
Source	SLS X06SA
Wavelength (Å)	1.00003
Resolution range (Å)	40.0 to 2.4
Unique reflections	11,676
Completeness (%)[a]	98.3 (97.1)
Multiplicity	8.5
$\langle I \rangle / \langle \sigma \rangle$[a]	20.8 (5.1)
R_{sym}[a,b]	5.8 (44.1)
Refinement	
Resolution range (Å)	20.0 to 2.4
Reflections used	11,676
Test set	584 (5%)
R_{cryst} (R_{free})[c,d]	24.3 (27.8)
Root mean square deviations	
Bond lengths (Å) / bond angles (degrees)	0.017/1.69
Average B factor (Å^2)[e]	67.0
Wilson B factor (Å^2)[e]	66.0
Ramachandran plot	
Percentage of residues in most favored/allowed/ generously allowed/forbidden regions	93.8/6.2/0/0
Non-hydrogen atoms	
Protein	1727
Water molecules	69

[a] Values in parentheses are for the highest resolution shell.
[b] $R_{sym}(I) = \Sigma_{hkl} \Sigma_i |I_i(hkl) - \langle I(hkl) \rangle| / \Sigma_{hkl} \Sigma_i I_i(hkl)$, where $\langle I(hkl) \rangle$ is the average intensity of the multiple $I_i(hkl)$ observations for symmetry-related reflections.
[c] $R_{cryst} = \Sigma_{hkl} ||F_o| - k|F_c|| / \Sigma_{hkl} |F_o|$.
[d] $R_{free} = \Sigma_{hkl \in T} ||F_o| - k|F_c|| / \Sigma_{hkl \in T} |F_o|$, where the test set ($T$ = 5% of reflections) is omitted in the refinement.
[e] The relatively high observed Wilson B-factor can be explained by a high crystal solvent content and few crystal contacts.

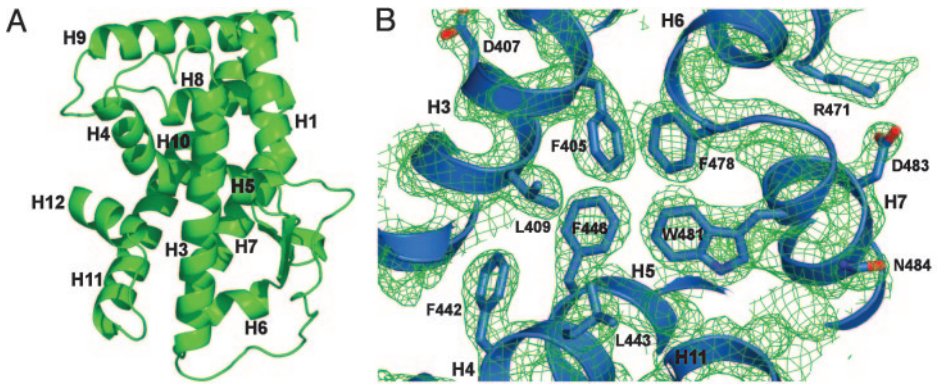

FIG. 1. **Overall structure of the NGFI-B LBD.** *A*, the NGFI-B LBD adopts an active conformation similar to ligand-activated NRs, as previously observed for Nurr1 and DHR38. *B*, the NGFI-B LBD does not contain a ligand-binding pocket. The available space is completely filled with bulky hydrophobic and aromatic residues. These residues are strictly conserved within the NR4 subfamily and adopt a conformation as found in the LBD structures of Nurr1 and DHR38 (Protein Data Bank code 1OVL and 1PDU, respectively).

positional deviation for the β-sheet, H7, and H10 and an approximately 1.5-Å shift of H12 relative to DHR38. Furthermore, the loop between H1 and H3, which is five amino acids longer in NGFI-B, adopts a conformation distinct from that in DHR38.

NGFI-B and Nurr1 Differ Significantly in the H11-H12 Region—Superimposition of the LBDs of NGFI-B and Nurr1 results in a root mean square deviation of 1.24 Å over 211 atoms (1.12 Å over 201 atoms for superimposition from H1 to H11). Both structures superimpose well in most parts of the LBD including loop regions, with the exception of H10, H11, and H12 (Fig. 2, *A* and *B*). Most interestingly, the Cα traces diverge increasingly from H11 to the C terminus of the LBD, such that H12 of NGFI-B is shifted by about 2.8 Å relative to H12 of Nurr1. The H12 shift is accompanied by a slight rotation along the helical axis. Further comparisons show that all three crystallized members of the subfamily (NGFI-B, Nurr1, and DHR38) diverge in the H12 region, although the H12 shift is most prominent for NGFI-B and Nurr1 (Fig. 2*D* and data not shown). These significant differences are unexpected given the high sequence conservation in the H11-H12 region of the three proteins (Fig. 2*E*). A detailed inspection of the crystal structures suggested that Met^{414} in H3 of Nurr1 (Leu^{413} in NGFI-B) may in part account for the H12 shift, since it is in contact with Ile^{587} in H12 (corresponding to Ile^{586} in NGFI-B) (Fig. 2, *A* and *B*). Alternatively, the methionine-to-leucine exchange in H3 may be secondary to other amino acid differences in the H11-H12 region, such as A586P or L591I (Nurr1 numbering).

However, the H11-H12 region of NGFI-B is involved in a crystal contact, which theoretically could also influence H12 positioning (Fig. 2*C*). The crystal contact covers a hydrophobic patch on the NGFI-B surface that is localized around Phe^{573} (H11) and Phe^{591} (H12). Strikingly, the H11-H12 regions of DHR38 and Nurr1 (three of six molecules present in the asymmetric unit (AU)) form a very similar crystal contact (Fig. 2*D*). H12 of the other three Nurr1 molecules in the AU is involved in a different crystal contact (data not shown). Superimposition of all six Nurr1 molecules reveals that the largest deviation between Cα atoms of H12 is around 1 Å (data not shown), suggesting that the crystal contacts have only a minor influence on

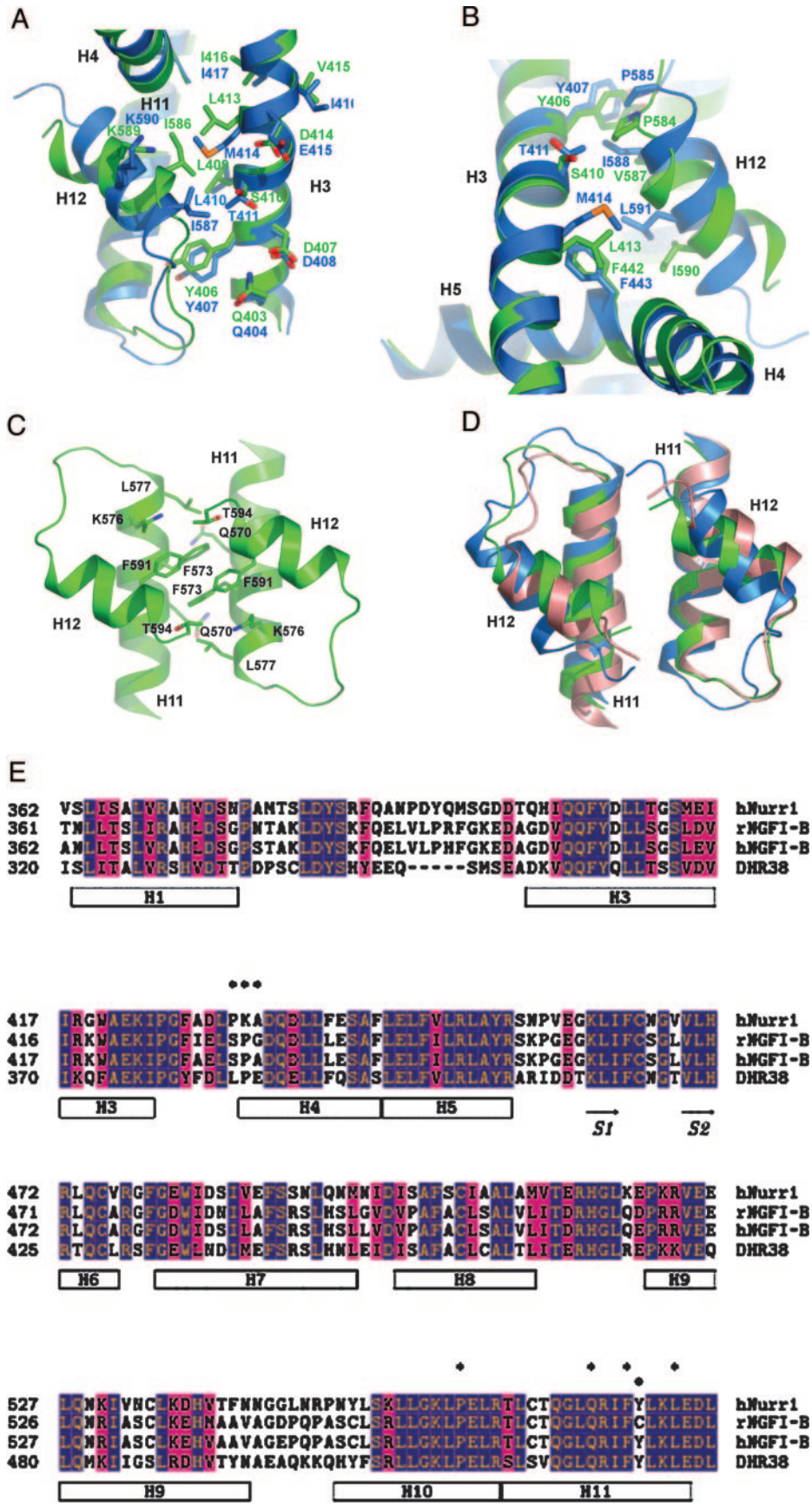

FIG. 2. **The LBDs of NGFI-B and Nurr1 diverge significantly in the H11-H12 region.** *A*, superimposition of selected parts of the LBDs of NGFI-B (*green*) and Nurr1 (*blue*). Whereas most regions superimpose well, both structures diverge from H11 to the C terminus, resulting in a slight rotation and a significant shift (about 2.8 Å) of H12. The H12 shift may in part be determined by the different size of Met^{414} (in H3 of Nurr1) and the corresponding Leu^{413} (in H3 of NGFI-B) that contact residues in H12 (Ile^{587} for Nurr1 and Ile^{586} for NGFI-B). *B*, local environment of Met^{414} in Nurr1 (*blue*). The side chain of Met^{414} contacts Ile^{587} (omitted for reasons of clarity) and Phe^{443}. Two other residues that are sensitive to mutation, Ile^{588} and Leu^{591} (12), cluster with Met^{414} in this spatially restricted region. Ile^{588} contacts Tyr^{407}, Thr^{411}, and Pro^{585}, whereas Leu^{591} interacts with Phe^{443}. The corresponding region of NGFI-B (*green*) has been superimposed. *C*, the H11-H12 region of NGFI-B is involved in a crystal contact shielding a hydrophobic patch on the LBD surface that involves Phe^{573} (H11) and Phe^{591} (H12). The crystal contact is unlikely to significantly perturb H12 positioning. *D*, the H11-H12 regions of NGFI-B (*green*), Nurr1 (*blue*) (three of six molecules found in the asymmetric unit), and DHR38 (*salmon*) form very similar crystal contacts. *E*, amino acid sequence alignment of human Nurr1, rat NGFI-B, human NGFI-B, and *Drosophila* DHR38. The secondary structure elements are given as observed for NGFI-B. Residues mutated in this study are marked by an *asterisk* or a *dot* for the swap mutants. *Blue*, conserved; *pink*, similar; *white*, nonconserved within the NR4A subfamily.

the position of H12. Visual inspection of the molecule packing in NGFI-B crystals supports the idea that the crystal contact formed by the H11-H12 region is unlikely to significantly perturb H12 positioning. Consequently, we reasoned that small but significant conservative exchanges in H3 or the H11-H12 region account for the H12 shift in NGFI-B relative to Nurr1, raising the question of whether the observed structural differences are related to specific functions.

A Specific H12 Position Determines the AF2 Activity of NGFI-B and Nurr1—Since the Nurr1 LBD exhibits potent activity in cell lines in which the AF2 of NGFI-B is only weakly active (12), we hypothesized that the distinct H12 positions might at least in part account for the different activation potentials. To evaluate the AF2 activity of Nurr1 and NGFI-B independently of the AF1 present in the N-terminal domain of both proteins, we generated a series of fusion proteins between the Gal4 DNA-binding domain and wild-type or mutant LBD of NGFI-B or Nurr1. First, we exchanged the H11-H12 region of Nurr1 for that of NGFI-B (mutant Gal4-Nurr1(Swap)) (Fig. 3*A*). This Nurr1 swap mutant contains six amino acid exchanges with respect to the wild-type receptor (Y575C, A586P, I588V, L591I, L593M, and P597S) (Fig. 2*E*). Three of these mutations are located on the LBD surface (Y575C, L593M, P597S), whereas the other three may influence H12 positioning: A586P, due to an increased rigidity of the proline residue, and I588V and L591I, since they are in contact with residues in H3, H4, or H11. To account for structural differences between NGFI-B and Nurr1 in H3, H12 was also swapped in the context of a M414L mutation (mutant Gal4-Nurr1(M414L-Swap)). Similarly, the corresponding NGFI-B swap mutants (Gal4-NGFI-B(Swap) and Gal4-NGFI-B(L413M-Swap)) were generated. To check if mutations in the loop between H3 and H4, that adopts a slightly different conformation in NGFI-B and Nurr1, affect the activity of the Nurr1 LBD, we replaced the residues with those of NGFI-B (mutant Gal4-Nurr1(P431S-K432P-A433G)). The replacement of the rigid Pro^{431} by serine or the introduction of a rigid proline and a flexible glycine at positions 432 and 433, respectively, might have a structural effect on the H3-H4 region and thus indirectly influence the position of H12.

The wild-type and mutant Gal4-LBD fusion proteins were tested in transient transfection assays in COS-1 cells on a $Gal4_{(3\times)}$TK-LUC reporter (Fig. 3*B*). Gal4-Nurr1 strongly activates transcription (about 40-fold), whereas the activity of Gal4-NGFI-B is only about 2–3-fold above base levels. Importantly, the activity of Gal4-Nurr1(Swap), and Gal4-Nurr1(M414L-Swap) is drastically reduced to approximately Gal4-NGFI-B levels, whereas the control mutant Gal4-Nurr1(P431S-K432P-A433G) appears to be slightly more active than the wild-type receptor. On the other hand, swapping the H12 region of Nurr1 into NGFI-B, in the context of the wild-type or mutant (L413M) receptor, generates proteins that are slightly (about 2-fold) more active than Gal4-NGFI-B.

These observations show that the H11-H12 regions of NGFI-B and Nurr1 are functionally not exchangeable and indicate that the transcriptional activity of these receptors may depend on a specific position of H12. In the case of NGFI-B, the swapped H11-H12 region of Nurr1 (even in the context of the L413M mutation) is apparently not sufficient to obtain full Nurr1-like activity. One possible explanation is that the LBD body of NGFI-B (H1-H11) does not precisely position the swapped H12 of Nurr1, irrespective of the presence of the L413M mutation. In the case of Nurr1, either an imprecise positioning or the distinct amino acid composition of the swapped H11-H12 region may account for the strongly reduced activity. To distinguish between these possibilities, we introduced a M414L, A586P, L591I, or L593M point mutation into Gal4-Nurr1 and a L413M control mutation into Gal4-NGFI-B. Of the six point mutations introduced into Nurr1 by swapping the H11-H12 region of rat NGFI-B, only three (A586P, L591I, or L593M) may be the functionally most relevant ones, because the other three are conserved between human NGFI-B and Nurr1 but differ in human and rat NGFI-B (Fig. 2*E*).

Introducing a M414L or a L591I mutation into Gal4-Nurr1 reduces the activity to about 35% of the wild-type receptor,

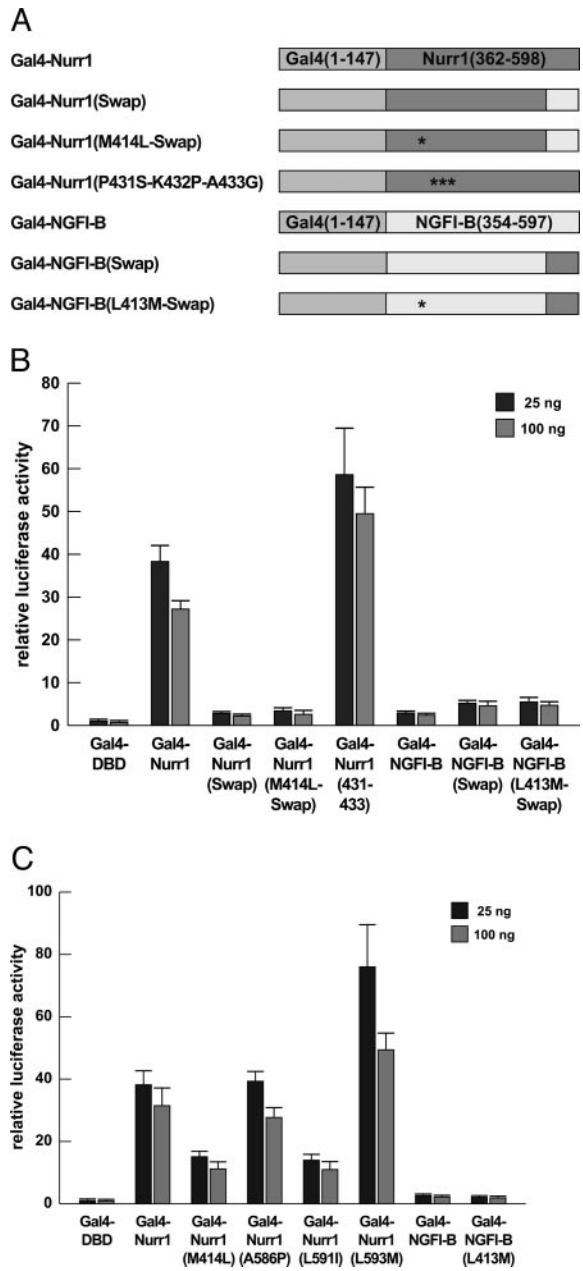

FIG. 3. **The activity of the Nurr1 LBD depends on a precisely positioned H12.** *A*, schematic representation of Nurr1 and NGFI-B swap mutants. The exchange of the H11-H12 region (swapped residues: 560–598 for Nurr1 and 559–597 for NGFI-B) results in six amino acid exchanges: Y575C, A586P, I588V, L591I, L593M, and P597S for Nurr1 and C574Y, P585A, V587I, I590L, M592L, and S596P for NGFI-B. *B* and *C*, transcriptional activity of wild-type and mutant Gal4-Nurr1 or Gal4-NGFI-B fusion proteins in transient transfection assays. COS-1 cells were transfected in 24-well plates with 250 ng of $Gal4_{(3\times)}$-TK-LUC reporter plasmid and 25 or 100 ng of the respective pCMX-Gal4-Nurr1 or pCMX-Gal4-NGFI-B expression plasmid per well. Luciferase activity was calculated relative to the pCMX-Gal4 control.

whereas the activity of Gal4-Nurr1(A586P) is not significantly decreased, and Gal4-Nurr1(L593M) is slightly more active than Gal4-Nurr1 (Fig. 3*C*). On the other hand, Gal4-NGFI-B and Gal4-NGFI-B(L413M) display comparable activities. Thus, point mutations, such as M414L or L591I, that are expected to influence H12 positioning significantly compromise the transcriptional activity of the Nurr1 LBD. Together, our results demonstrate a strong sensitivity of H12 to positional changes suggesting its direct rather than indirect involvement in transcriptional activation.

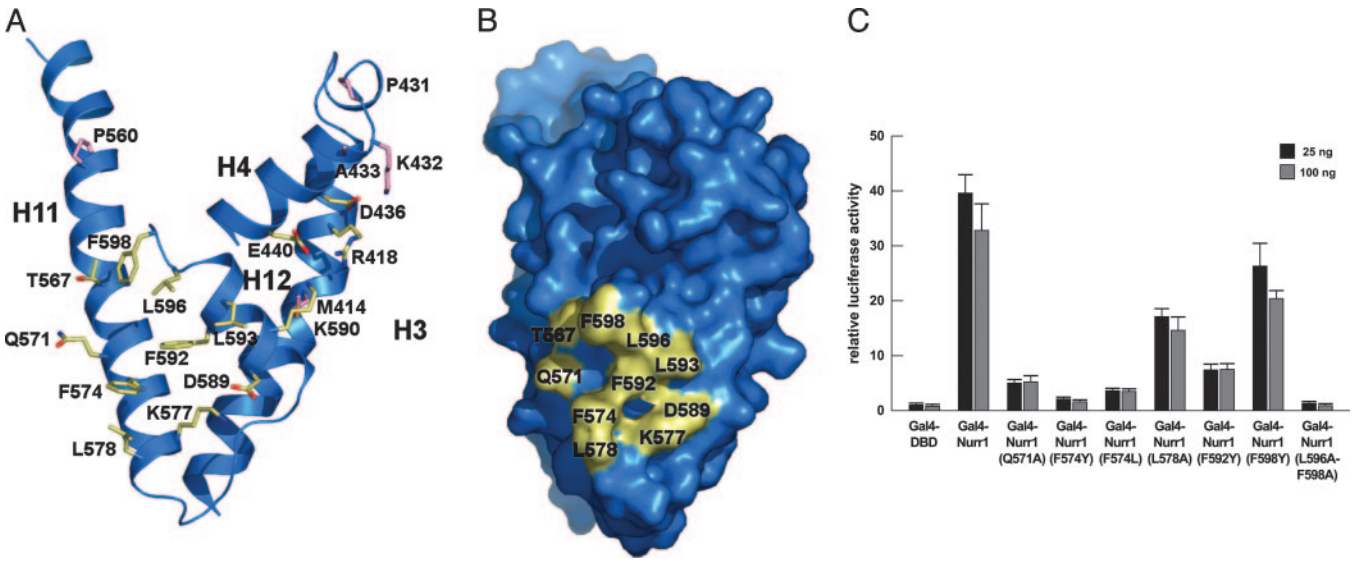

FIG. 4. **The cell type-dependent AF2 activity of Nurr1 depends on a novel co-regulator surface.** *A*, representation of two potential co-regulator surfaces in the Nurr1 LBD. The canonical surface found in ligand-regulated NRs is constituted by H3, H4, and H12 but has been shown not to contribute to the AF2 activity of Nurr1 (27). The novel co-regulator surface is determined by a specific H12 position and constituted by residues of H11 and H12. Selected residues that contribute to the surfaces are depicted. *B*, topology of the novel co-regulator surface constituted by the H11-H12 region. Implicated residues are *colored yellow*. *C*, mutation of residues that constitute the novel co-regulator surface reduces the activity of the Nurr1 LBD. Transient transfection of COS-1 cells using wild-type and mutant Gal4-Nurr1 fusion proteins was performed as described in Fig. 3, *B* and *C*.

The Cell Type-dependent Activity of the Nurr1 LBD Depends on a Novel Co-regulator Surface—Several previous studies focused on the role of H12 for Nurr1 activity (12, 22, 27, 34). Since mutations in the canonical co-activator cleft constituted by H3, H4, and H12 do not significantly influence the activity of the Nurr1 LBD (27), we considered an alternative surface, to which H12 directly contributes and which should be sensitive to mutation. H11, H12, and the connecting loop between both helices constitute the only plausible alternative (Fig. 4, *A* and *B*). As noted before, this hydrophobic surface forms very similar contacts in crystals of the NGFI-B, Nurr1, and DHR38 LBD (Fig. 2, *C* and *D*). To test the role of this putative co-regulator interface in AF2 activity, we assayed a series of point mutants (Q571A, F574Y, F574L, L578A, F592Y, F598Y, and L596A/F598A) in the context of Gal4-Nurr1 (Fig. 4*C*). It is important to note that mutations were chosen such that they are unlikely to destabilize the entire LBD or to disrupt interactions between H12 and the LBD body.

As shown in Fig. 4*C*, the activity of the mutants F574Y and L596A/F598A is almost completely abolished, whereas Q571A, F574L, and F592Y retain some activity. In comparison, the mutants L578A and F598Y activate transcription with about 50% of wild-type receptor efficiency. These results provide strong evidence for a direct role of the surface constituted by the H11-H12 region (notably residues Phe^{574}, Phe^{592}, and Leu^{596}) in Nurr1 transcriptional activation. Phe^{598} may be located at the border of the co-regulator surface such that a F598Y mutation does not significantly disturb its hydrophobic character.

Heterodimerization with RXR Does Not Compromise the Activity of the Nurr1 LBD—Modulation of the activity of full-length Nurr1 by unliganded RXR on NGFI-B response elements has been observed previously (46). Since mutation of Leu^{596} and Phe^{598} at the C terminus of the LBD compromises Nurr1 activity, we asked whether heterodimerization with RXR could negatively influence the activity of the AF2. Assuming the formation of a canonical RXR-Nurr1 LBD heterodimer similar to those observed for the LBDs of RXRα-RARα (47) or RXRα-peroxisome proliferator-activated receptor γ (48), the RXR surface might contact the C terminus and thus modulate the activity of the Nurr1 LBD (Fig. 5*A*). To test this hypothesis, we co-expressed in COS-1 cells Gal4-Nurr1, Gal4-Nurr1(L596A/F598A) or Gal4-Nurr1(P560E) with full-length RXRα or RXRα fused to the VP16 activation domain in the absence or presence of the RXR agonist BMS649 (Fig. 5*B*). The P560E mutation is expected to disrupt RXR-Nurr1 heterodimer formation like the previously reported P560A mutation (46).

In the absence of ligand, increasing amounts of RXRα do not influence the activity of Gal4-Nurr1 (Fig. 5*B*). Under these conditions, the addition of BMS649 results in a small (about 2-fold) increase in activity. In comparison, reporter gene transcription is strongly stimulated upon the co-expression of VP16-RXRα suggesting heterodimer formation. The low basal activity of Gal4-Nurr1(L596A/F598A) is not influenced by apo-RXR and about 2-fold increased by RXRα stimulated with BMS649, whereas co-expression of VP16-RXRα results in higher transcriptional activity of the complex. On the other hand, the (close to wild-type) activity of Gal4-Nurr1(P560E) is not influenced by apo- or holo-RXRα and modestly augmented upon co-expression of VP16-RXRα. We note, however, that dimerization of Gal4-Nurr1(P560E) with RXRα is apparently not completely abolished. Together, these observations suggest that mutation of the C terminus of Nurr1 does not significantly influence heterodimer formation and that interaction with RXR does not compromise the AF2 activity of Nurr1.

DISCUSSION

In this study, we present the crystal structure of the NGFI-B LBD at 2.4-Å resolution in combination with functional studies on NGFI-B and Nurr1. Like the LBDs of Nurr1 and DHR38 (27, 28), the NGFI-B LBD adopts an active conformation in the absence of a functional ligand-binding pocket, since large aromatic or hydrophobic residues completely fill the available space. Overall, the NGFI-B LBD superimposes well with the LBDs of DHR38 and Nurr1. Positional shifts of up to 1.5 Å for individual helices including H12 are observed between NGFI-B and DHR38, and also DHR38 and Nurr1 differ in the H11-H12 region (data not shown) (49). Most relevant for this work, the structures of NGFI-B and Nurr1 diverge increasingly in the

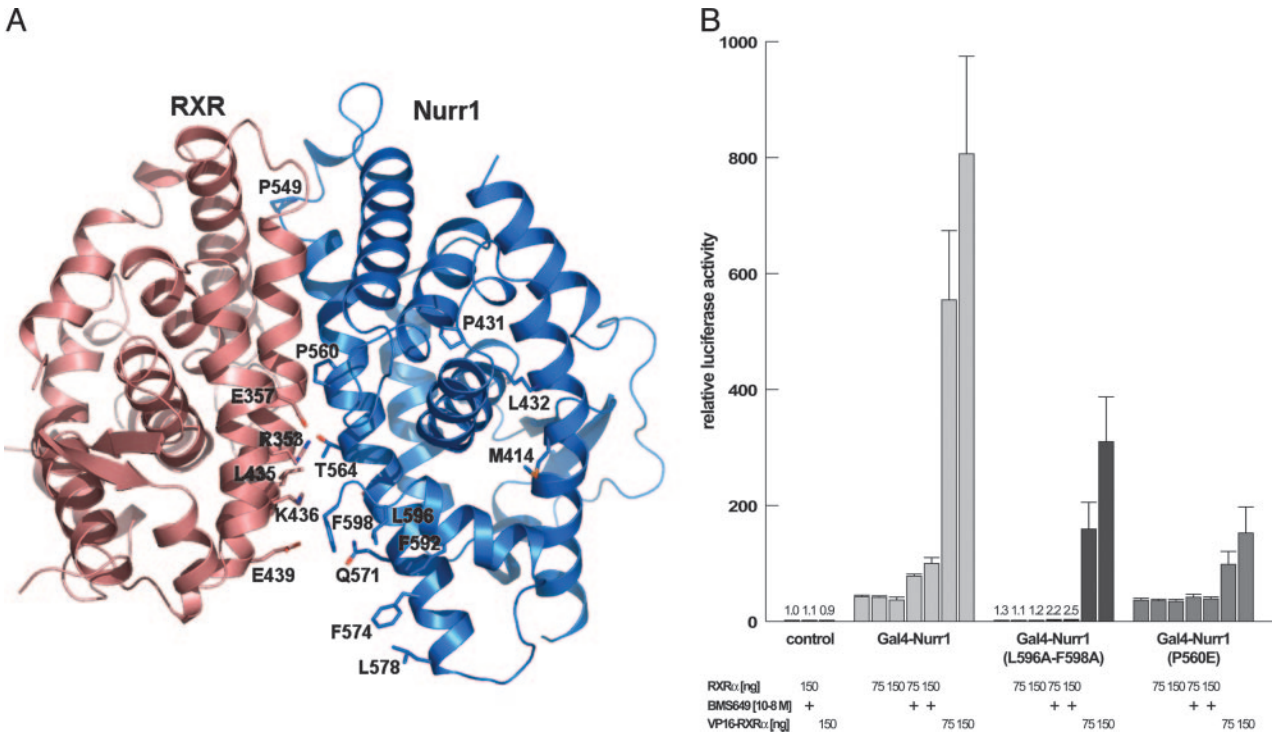

FIG. 5. **Heterodimerization with RXR does not influence the cell type-dependent activity of the Nurr1 LBD.** *A*, heterodimer model of the LBDs of RXR and Nurr1. The RXR-RAR LBD crystal structure (Protein Data Bank code 1DKF) was used as a template, and the Nurr1 LBD was globally superimposed with the RAR LBD. Assuming that Nurr1 and RAR heterodimerize with RXR in a similar manner, either heterodimerization or the AF2 activity of Nurr1 might be affected by contacts between the Nurr1 C terminus and the RXR LBD. *B*, transcriptional activity of Gal4-Nurr1, Gal4-Nurr1(L596A/F598A), and Gal4-Nurr1(P560E) upon co-transfection of different amounts (75 or 150 ng/well) of pCMX-RXRα or pCMX-VP16-RXRα expression plasmid in the absence or presence of 10^{-8} M RXR agonist (BMS649). Mutation of P560 to glutamate is expected to interfere with RXR heterodimer formation. COS-1 cells were transfected as described in Fig. 3, *B* and *C*.

H11-H12 region, resulting in a relative H12 shift of about 2.8 Å (Fig. 2, *A* and *B*), which is unexpected from the high sequence similarity (Fig. 2*E*). Strikingly, the H11-H12 regions of NGFI-B, DHR38, and Nurr1 (three of six molecules present in the AU) are involved in very similar crystal contacts that shield a hydrophobic patch on the LBD surface (Fig. 2, *C* and *D*). Due to the involvement in crystal packing, it is not possible to draw immediate conclusions about the distinct H12 positioning, since the crystal contacts could theoretically be responsible for the observed shifts. Visual inspection of the NGFI-B LBD crystal packing suggests that the H11-H12 contact is unlikely to significantly influence H12 positioning. More importantly, superimposition of the six LBD molecules present in the AU of Nurr1 crystals (27) reveals only minor H12 deviations to maximally 1 Å, suggesting that factors other than crystal packing determine the significant 2.8-Å shift of H12 of NGFI-B relative to Nurr1. We therefore aimed at determining the structural basis and the functional consequences of this H12 shift and asked whether it accounts for the distinct, cell type-dependent activities of the NGFI-B and the Nurr1 LBD (12).

A detailed comparison of the crystal structures suggests that conservative amino acid exchanges in H3 (Met^{414} in Nurr1 corresponding to Leu^{413} in NGFI-B) or the H11-H12 region may partly account for the distinct H12 positions and transcriptional activities. Accordingly, exchanging the H11-H12 region of (human) Nurr1 for that of (rat) NGFI-B (*i.e.* introducing six point mutations) dramatically compromises the activity of the Nurr1 LBD, showing that this region is functionally not equivalent in both receptors (Fig. 3*B*). Three of these mutations (A586P, I588V, and L591I) may influence H12 positioning, whereas L593M and P597S may affect the novel co-regulator surface identified in this study (discussed below), and Y575C may not significantly alter Nurr1 activity, since the side chain points away from the novel co-regulator surface. Interestingly, only three amino acids differ in the H11-H12 region of Nurr1 and human NGFI-B (A586P, L591I, and L593M (Fig. 2*E*)), indicating that these might be the functionally more relevant ones.

Examination of the effect of single amino acid exchanges on Nurr1 transactivation shows that the mutants M414L (in H3) and L591I (in H12) exhibit about 35% of wild-type receptor activity, whereas mutation of Ala^{586} to proline or of Leu^{593} (in the novel co-regulator surface) to methionine does not reduce activity (Fig. 3*C*). These observations support the idea that the distinct transcriptional activities of the NGFI-B and the Nurr1 LBD may, in part, be caused by small changes in H12 positioning due to conserved amino acid exchanges in H3 and H12. Two previously reported Nurr1 mutants with strongly reduced activity (I588A and L591A) (12) fall into the same category as M414L and L591I. Ile^{588} (H12) forms hydrophobic contacts with the side chains of Tyr^{407} (H3), Thr^{411} (H3), and Pro^{585} (H11-H12 loop), whereas Leu^{591} (H12) is in contact with Phe^{443} (in the kink between H4 and H5). Interestingly, the side chain of Met^{414} (H3) also contacts Phe^{443}. Thus, Met^{414}, Ile^{588}, and Leu^{591} cluster in a spatially restricted region that is apparently very sensitive to mutation (Fig. 2*B*).

In the case of the reverse swap, replacement of the H11-H12 region of NGFI-B by that of Nurr1 (in the presence or absence of a L413M mutation) modestly increases the activity of the mutant receptor. We hypothesize that these mutants do not gain full Nurr1-like activity, because the swapped H12 region cannot be precisely positioned due to other small structural differences of the NGFI-B LBD body. Together, these results show that a specific H12 position determines the AF2 activities of NGFI-B and Nurr1 and suggest that H12 is directly rather than indirectly involved in transactivation, raising the question of the location of a co-regulator surface that contains H12

but differs from the canonical one.

Previous studies have shown that H12 is essential for the transcriptional activity of the Nurr1 LBD, since its deletion abolishes the activity of the receptor (12, 34). Effects of point mutations on Nurr1 AF2 activity have mainly been attributed to a disruption of interactions between H12 and the LBD body (12, 27). Mutants that were hypothesized to fall into this category are D589A (H12), breaking the salt bridge with Lys^{577} (H11), and F592A (H12), disrupting hydrophobic contacts with Phe^{574} (H11) (27). Other point mutations were generated to assess the potential role of the canonical H3-H4-H12 surface for Nurr1 activity. Since mutations such as R418V (H3), E440K (H4), R454E (H5), or K432I/D436I (H4) do not significantly influence the activity of the Nurr1 LBD (27), the canonical surface is apparently not involved in AF2 functioning. Consistently, the hydrophilic rather than hydrophobic character of the H3-H4-H12 surface, which does not permit the recruitment of L*XX*LL-containing co-activators, has been documented (25, 27). Finally, based on the observation that Nurr1 LBD stability may depend on the cell type or be regulated by the tyrosine kinase Ret, as assessed by an LBD assembly assay (50), it was proposed that Nurr1 activity may be correlated with regulated, ligand-independent stabilization of the LBD (27). However, this idea did not clarify the location of a putative co-regulator surface. Furthermore, questions remained of whether the effects of several point mutations on Nurr1 activity were convincingly explained. The orientation of the side chain of Phe^{592} (H12), for example, allows only weak hydrophobic contacts with Phe^{574} (H11), and the side chain of Leu^{593} (H12) is located on the surface and probably not involved in H12 positioning. Nevertheless, mutation of these residues to alanine affects Nurr1 activity (12). Finally, it was not clear why disruption of the salt bridge between Asp^{589} (H12) and Lys^{577} (H11) reduces Nurr1 activity, whereas disruption of another salt bridge between Lys^{590} (H12) and Glu^{440} (H4) (pointing toward the canonical H3-H4-H12 surface) has no significant effect (12).

Our observations discussed above and these unexplained mutant effects strongly suggested that the hydrophobic surface constituted by H11, the H11-H12 loop, and H12 (to which Lys^{577}, Asp^{589}, Phe^{592}, and Leu^{593} contribute) plays a direct role in Nurr1 transactivation (Fig. 4, *A* and *B*). In agreement with this idea, we show that mutation of surface residues in this region affects Nurr1 AF2 activity (Fig. 4*C*). Importantly, phenylalanine residues were mutated to tyrosine to avoid potential disruption on even weak hydrophobic interactions with neighboring side chains. The relative activities of the mutants and their position on the surface suggest that Gln^{571}, Phe^{574}, Phe^{592}, and the previously mutated Leu^{593} and Asp^{589} (12) together with Lys^{577} and possibly Leu^{596} contribute directly to the novel co-regulator surface. Phe^{598} may be located at its border, and Leu^{578} may contribute either directly or indirectly by stabilizing the position of Phe^{574}, which possibly explains the smaller effect of the mutants F598Y and L578A.

Despite the presumed proximity of C-terminal residues that are involved in the novel co-regulator surface to the RXR surface, under our experimental conditions heterodimerization with RXR has no apparent influence on the AF2 activity of Nurr1. This observation indicates that the reported modulation of the activity of full-length Nurr1 by unliganded RXR on NGFI-B response elements (46) may not depend on the Nurr1 LBD.

While this manuscript was in preparation, Codina *et al.* (49) also identified the novel co-regulator surface using NMR footprinting to map peptide binding to the Nurr1 LBD. The authors observe weak binding of NCoR and SMRT co-repressor fragments to this surface *in vitro* and show that binding of a SMRT fragment to the Nurr1 mutants F574A (H11), F592A (H12), and L593A (H12) is reduced. However, their study leaves several open questions. First, in this and previous studies (12, 27), only alanine mutants were generated. Since mutation of Phe^{574} (H11) or Phe^{592} (H12) to alanine may destabilize H12 positioning by interfering with hydrophobic interactions (27), we assayed the activity of the corresponding tyrosine or leucine mutants (F574Y, F574L, F592Y) (Fig. 4*C*). Next, only one H11 mutant (F574A) was generated and tested *in vitro* (49). Therefore, our *in vivo* results for F574Y, F574L, and two additional H11 mutants (Q571A and L578A) provide a more complete picture on the novel co-regulator surface. Finally, since SMRT was reported previously to negatively regulate the activity of NGFI-B (22) rather than Nurr1, the functional relevance of co-repressor binding to the transcriptional activator Nurr1 remained unclear. Importantly, Codina *et al.* (49) did not address the question of why NGFI-B does not activate transcription as efficiently as Nurr1, although all identified residues that contribute to the novel co-regulator surface are conserved with the exception of Leu^{593} (Met^{592} in NGFI-B). As shown in Fig. 3*C*, this amino acid difference does not account for the distinct AF2 activities of NGFI-B and Nurr1.

The significant relative H12 shift in the NGFI-B LBD provides plausible explanations for open questions and supports a simple model in which the AF2 activity of NGFI-B and Nurr1 is determined by co-repressors such as SMRT or NCoR and yet to be identified co-activators. Due to the structural differences, co-activators would bind with high relative affinity to the novel co-regulator surface on the Nurr1 LBD, whereas co-repressors would preferentially be recruited to the corresponding surface on the NGFI-B LBD. Accordingly, the relative protein levels of co-activator and co-repressor would determine the cell type-dependent transcriptional activity of the AF2 of Nurr1 and NGFI-B. This idea implies the possibility that co-factor recruitment can be regulated by, for example, phosphorylation of the LBD body, which in turn could influence H12 positioning.

In summary, our structural and functional comparison of the LBDs of NGFI-B and Nurr1 suggests that a specifically positioned H12 that contributes directly to a novel co-regulator surface determines the cell type-dependent AF2 activities of NGFI-B and Nurr1.

Acknowledgments—We thank Hiroshi Ichinose for the gift of the plasmids pET-15b-Nurr1 and pET-15b-NGFI-B and Roland Schüle for providing the plasmids pCMX-RXRα and pCMX-VP16-RXRα. We are grateful to Virginie Chavant for technical assistance, Hélène Nierengarten for mass spectrometry analysis, André Mitschler for help with crystal preparation and testing, Bruno Klaholz for critical reading of the manuscript, and Clemens Schulze-Briese and Armin Wagner for help with data collection at the Swiss Light Source (Villigen).

REFERENCES

1. The Nuclear Receptor Nomenclature Committee (1999) *Cell* **97,** 161–163
2. Paulsen, R. F., Granas, K., Johnsen, H., Rolseth, V., and Sterri, S. (1995) *J. Mol. Neurosci.* **6,** 249–255
3. Maruyama, K., Tsukada, T., Ohkura, N., Bandoh, S., Hosono, T., and Yamaguchi, K. (1998) *Int. J. Oncol.* **12,** 1237–1243
4. Sutherland, J. D., Kozlova, T., Tzertzinis, G., and Kafatos, F. C. (1995) *Proc. Natl. Acad. Sci. U. S. A.* **92,** 7966–7970
5. Wilson, T. E., Fahrner, T. J., and Milbrandt, J. (1993) *Mol. Cell. Biol.* **13,** 5794–5804
6. Maira, M., Martens, C., Philips, A., and Drouin, J. (1999) *Mol. Cell. Biol.* **19,** 7549–7557
7. Forman, B. M., Umesono, K., Chen, J., and Evans, R. M. (1995) *Cell* **81,** 541–550
8. Perlmann, T., and Jansson, L. (1995) *Genes Dev.* **9,** 769–782
9. Zetterstrom, R. H., Solomin, L., Mitsiadis, T., Olson, L., and Perlmann, T. (1996) *Mol. Endocrinol.* **10,** 1656–1666
10. Law, S. W., Conneely, O. M., DeMayo, F. J., and O'Malley, B. W. (1992) *Mol. Endocrinol.* **6,** 2129–2135
11. Murphy, E. P., Dobson, A. D., Keller, C., and Conneely, O. M. (1996) *Gene Expr.* **5,** 169–179
12. Castro, D. S., Arvidsson, M., Bondesson Bolin, M., and Perlmann, T. (1999) *J. Biol. Chem.* **274,** 37483–37490
13. Liu, Z. G., Smith, S. W., McLaughlin, K. A., Schwartz, L. M., and Osborne,

B. A. (1994) *Nature* **367,** 281–284
14. Cheng, L. E., Chan, F. K., Cado, D., and Winoto, A. (1997) *EMBO J.* **16,** 1865–1875
15. He, Y. W. (2002) *J. Leukocyte Biol.* **72,** 440–446
16. Ethier, I., Beaudry, G., St-Hilaire, M., Milbrandt, J., Rouillard, C., and Levesque, D. (2004) *Neuropsychopharmacology* **29,** 335–346
17. Zetterstrom, R. H., Solomin, L., Jansson, L., Hoffer, B. J., Olson, L., and Perlmann, T. (1997) *Science* **276,** 248–250
18. Saucedo-Cardenas, O., Quintana-Hau, J. D., Le, W. D., Smidt, M. P., Cox, J. J., De Mayo, F., Burbach, J. P., and Conneely, O. M. (1998) *Proc. Natl. Acad. Sci. U. S. A.* **95,** 4013–4018
19. Le, W. D., Xu, P., Jankovic, J., Jiang, H., Appel, S. H., Smith, R. G., and Vassilatis, D. K. (2003) *Nat. Genet.* **33,** 85–89
20. Ohkura, N., Hijikuro, M., Yamamoto, A., and Miki, K. (1994) *Biochem. Biophys. Res. Commun.* **205,** 1959–1965
21. Pekarsky, Y., Hallas, C., Palamarchuk, A., Koval, A., Bullrich, F., Hirata, Y., Bichi, R., Letofsky, J., and Croce, C. M. (2001) *Proc. Natl. Acad. Sci. U. S. A.* **98,** 3690–3694
22. Sohn, Y. C., Kwak, E., Na, Y., Lee, J. W., and Lee, S. K. (2001) *J. Biol. Chem.* **276,** 43734–43739
23. Kovalovsky, D., Refojo, D., Liberman, A. C., Hochbaum, D., Pereda, M. P., Coso, O. A., Stalla, G. K., Holsboer, F., and Arzt, E. (2002) *Mol. Endocrinol.* **16,** 1638–1651
24. Slagsvold, H. H., Ostvold, A. C., Fallgren, A. B., and Paulsen, R. E. (2002) *Biochem. Biophys. Res. Commun.* **291,** 1146–1150
25. Wansa, K. D., Harris, J. M., and Muscat, G. E. (2002) *J. Biol. Chem.* **277,** 33001–33011
26. Maira, M., Martens, C., Batsche, E., Gauthier, Y., and Drouin, J. (2003) *Mol. Cell. Biol.* **23,** 763–776
27. Wang, Z., Benoit, G., Liu, J., Prasad, S., Aarnisalo, P., Liu, X., Xu, H., Walker, N. P., and Perlmann, T. (2003) *Nature* **423,** 555–560
28. Baker, K. D., Shewchuk, L. M., Kozlova, T., Makishima, M., Hassell, A., Wisely, B., Caravella, J. A., Lambert, M. H., Reinking, J. L., Krause, H., Thummel, C. S., Willson, T. M., and Mangelsdorf, D. J. (2003) *Cell* **113,** 731–742
29. Galleguillos, D., Vecchiola, A., Fuentealba, J. A., Ojeda, V., Alvarez, K., Gomez, A., and Andres, M. E. (2004) *J. Biol. Chem.* **279,** 2005–2011
30. Song, K. H., Park, Y. Y., Park, K. C., Hong, C. Y., Park, J. H., Shong, M., Lee, K., and Choi, H. S. (2004) *Mol. Endocrinol.* **18,** 1929–1940
31. Greschik, H., and Moras, D. (2003) *Curr. Top. Med. Chem.* **3,** 1573–1599
32. Darimont, B. D., Wagner, R. L., Apriletti, J. W., Stallcup, M. R., Kushner, P. J., Baxter, J. D., Fletterick, R. J., and Yamamoto, K. R. (1998) *Genes Dev.* **12,** 3343–3356
33. Nolte, R. T., Wisely, G. B., Westin, S., Cobb, J. E., Lambert, M. H., Kurokawa, R., Rosenfeld, M. G., Willson, T. M., Glass, C. K., and Milburn, M. V. (1998) *Nature* **395,** 137–143
34. Castillo, S. O., Xiao, Q., Kostrouch, Z., Dozin, B., and Nikodem, V. M. (1998) *Gene Expr.* **7,** 1–12
35. Kabsch, W. (1993) *J. Appl. Crystallogr.* **26,** 795–800
36. Navaza, J. (1994) *Acta Crystallogr. Sect. A* **50,** 157–163
37. Brunger, A. T., Adams, P. D., Clore, G. M., DeLano, W. L., Gros, P., Grosse-Kunstleve, R. W., Jiang, J. S., Kuszewski, J., Nilges, M., Pannu, N. S., Read, R. J., Rice, L. M., Simonson, T., and Warren, G. L. (1998) *Acta Crystallogr. Sect. D* **54,** 905–921
38. Collaborative Computational Project Number 4 (1994) *Acta Crystallogr. Sect. D* **50,** 760–763
39. Murshudov, G. N. (1997) *Acta Crystallogr. Sect. D* **53,** 240–255
40. Potterton, E., Briggs, P., Turkenburg, M., and Dodson, E. (2003) *Acta Crystallogr. Sect. D* **59,** 1131–1137
41. Perrakis, A., Harkiolaki, M., Wilson, K. S., and Lamzin, V. S. (2001) *Acta Crystallogr. Sect. D* **57,** 1445–1450
42. Jones, T. A., Zou, J. Y., Cowan, S. W., and Kjeldgaard, M. (1991) *Acta Crystallogr. Sect. A* **47,** 110–119
43. Laskowski, R. A., MacArthur, M. W., Moss, D. S., and Thornton, J. M. (1993) *J. Appl. Crystallogr.* **26,** 283–291
44. DeLano, W. L. (2002) *The PyMOL Molecular Graphics System*, DeLano Scientific LLC, South San Francisco, CA
45. Beitz, E. (2000) *Bioinformatics* **16,** 135–139
46. Aarnisalo, P., Kim, C. H., Lee, J. W., and Perlmann, T. (2002) *J. Biol. Chem.* **277,** 35118–35123
47. Bourguet, W., Vivat, V., Wurtz, J. M., Chambon, P., Gronemeyer, H., and Moras, D. (2000) *Mol. Cell* **5,** 289–298
48. Gampe, R. T., Jr., Montana, V. G., Lambert, M. H., Miller, A. B., Bledsoe, R. K., Milburn, M. V., Kliewer, S. A., Willson, T. M., and Xu, H. E. (2000) *Mol. Cell* **5,** 545–555
49. Codina, A., Benoit, G., Gooch, J. T., Neuhaus, D., Perlmann, T., and Schwabe, J. W. (2004) *J. Biol. Chem.* **279,** 53338–53345
50. Pissios, P., Tzameli, I., Kushner, P., and Moore, D. D. (2000) *Mol. Cell* **6,** 245–253